Towards variable impedance assembly: the VSA peg-in-hole

Leonardo Balletti[1,4], Alessio Rocchi[1,4], Felipe Belo[1,3] Manuel Catalano[1,2,3]
Manolo Garabini[1,3], Giorgio Grioli[1,3] and Antonio Bicchi[1,2,3]

***Abstract*—This paper shows how an accurate peg-in-hole assembly task can be easily achieved with nothing but cheap position sensors when resourcing to Variable Impedance Actuators (VIA). We present the use of a low-cost Variable Stiffness Torso platform, that consists of two 4-DOF non-planar VSA manipulators, for a peg-in-hole assembly task using both arms. One arm holds the peg and the other holds the hole. The task is accomplished without any force measurement and without calling for parallel-manipulator control techniques, exploiting the intrinsic mechanical elasticity of the actuator units. Indeed, a simple position control scheme is required. Simulations and experimental results are reported.**

I. Introduction

Robotic assembly, already commonplace in industrial manufacturing, could be taken to a whole new level by employing Variable Impedance Actuators (VIA). The current generation of industrial manipulators is mainly applied to repetitive factory operations or to the production of artificial, cold and sterile objects. They require high precision, even for the execution of the simplest tasks, at the cost of the use of expensive hardware, sensors and the application of advanced control techniques. On the other hand, the authors believe that VIA technology will propel the next generation of assembly robots and support this idea by presenting a compelling demonstration of its possibilities.

While VIA robots exceed on performing human-like chores, early VIA studies investigated industrial scenarios, specifically those where humans and robots must cooperate. Indeed, variable impedance can be put to good use in order to guarantee safety in human-robot interaction as first demonstrated by the safe brachistochrone problem (a minimum time rest to rest position task under a safety constraint) in [1]. Another very recent work shows interest in the use of VIA robots for industrial duties, more specifically for peg-in-hole like assembly tasks [2]. While this work only addresses the two dimensional problem and uses a very simplistic framework, i.e. a 3-DOF planar manipulator assembling a peg to fixed hole, it shows a clever approach to the assembly problem and underlines the intrinsic performance gain of passive compliance against active impedance control at high frequencies. Moreover recently a control approach combining the two paradigms of VSA and active impedance control has been developed [3]. Historically the peg-in-hole task has been researched extensively [4], both for quasi-static and dynamic insertion cases. Especially for the second case passive compliances are considered the best solution [5] to avoid insertion problems (jamming and wedging), with classic passive methods like the RCC and its variants resulting unsuitable for difficult assemblies [6]. While compliance control in its forms of simple force control [7], hybrid position-force control [8], active impedance control [9], passive compliance [10], sensor-less trajectory search [6] deal mainly with the assembly insertion problem with the scope of completing faster and faster assemblies without jamming and wedging, search strategies for hole localization and misalignment reductions are also important. Several methods exist to cope with uncertainties: space search [11] and force feedback, reinforcement learning [12], vision [13], combined sensing and randomization [14].

Fig. 1. The CubeBot, a 13 DOF VSA bi-manual torso, executing a peg-in-hole task. A pre-insert position is shown in the picture.

It has already been recognized by the research community that VIA permits robots to achieve higher performance in terms of energy efficiency [15], [16], speed [17]–[20], robustness [21] and task adaptability [22]. VIA robots outshine conventional robots with unparalleled human-like grace and dexterity, as it has been demonstrated by recent works that exploit VIA characteristics on the accomplishment of common human tasks that still present a challenge for tradi-

[1]Centro Interdipartimentale di Ricerca "E. Piaggio", Università di Pisa, 1 Largo L. Lazzarino, 56100 Pisa, Italy.
[2]Advanced Robotics Department, Italian Institute of Technology, 30 Via Morego, 16163 Genova, Italy.
[3] {felipe.belo,manuel.catalano,manolo.garabini, giorgio.grioli,bicchi}@centropiaggio.unipi.it
[4]First two authors appear in alphabetical order.

tional robots. For example, while humans take running and jumping for granted, these are complex dynamic tasks that can be tackled using variable stiffness as investigated in [23]. Likewise, grasping is still a popular research topic that can benefit from variable stiffness [24]. Many other specific and original demonstrations of VIA application were also shown lately: [18] and [17] investigate the use of variable stiffness for speed optimization during hammering and kicking tasks, respectively, in [22] a VSA robot is controlled to hold a pen and draw a circle in an uneven surface and [25] shows a VSA playing darts.

Despite the VIA field growing mature in terms of design, implementation and control techniques, former findings demonstrate that its expansion is way far from slowing down. Moreover those many unexplored application fields often hint for unexploited aspects and peculiarity of the technology itself. Aspects of a VIA dynamic behavior which were considered as drawbacks by some, are rather gaining the status of *feature*. One of these aspects surely is the intrinsic non-linearity which fundamentally belongs to most VIA actuators. Perceived as an annoying deviation from a linear, easily predictable, behavior, nowadays is appreciated as a stiffness self-modulation capability. This has the effect to produce a smooth transition toward higher levels of impedance as the deformation from the unloaded equilibrium position grows more pronounced. Such *embedded behavior* has the advantage of protecting the actuator from abrupt load variations on one side and, more importantly, on the other side, it dynamically re-maps the power exerted by the actuator onto the load. Thus if a configuration of loose coupling is used for finer force control with a lower load, a load increase yields a tighter coupling which allows for faster transfer of power to the load, thus a prompter position control.

In this paper the intrinsic adaptivity offered by impedance non-linearity is exploited to execute a blind peg-in-hole assembly task. The use of variable stiffness actuators permitted us to solve the problem using a simple straightforward position-control approach, without resourcing to any complex higher order dynamic control schemes, force sensors, and high-cost precise manipulators. As far as we know this is the first work to present the use of VSA non-planar manipulators for the accomplishment of the peg-in-hole assembly task. It is also the first to do so using two VSA manipulators, one holding the peg, and the other holding the hole. In our solution the parallel task is remapped to an equivalent serial task by parameterizing the two arms as one 8-DOF serial manipulator [26], [27]. Moreover, algorithms for searching the hole and performing the insertion using only position feedback are discussed. Finally, the proposed solution is validated with both simulations and experimental results.

In Section II the task is defined, while in Section III the search and insertion strategy is presented. Finally, in Section IV experimental results are given.

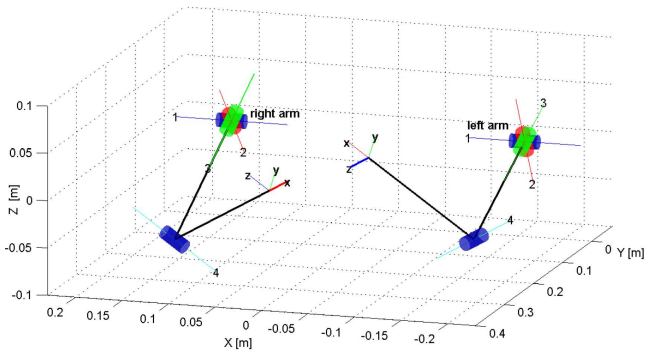

Fig. 2. Scheme of the Kinematic model for both arms. Rotation axes are numbered, with positive direction facing away from the numbers

II. Problem Definition

A. Kinematics

Consider a robot, as the one shown in Fig. 1, with two arms, each having a model whose kinematics is described by DH table I.

Joint	a	α	d	θ
1	0	$-\frac{\pi}{2}$	0	q_1
2	0	$\frac{\pi}{2}$	0	$q_2+\frac{\pi}{2}$
3	0	$\frac{\pi}{2}$	$-d_3$	$q_3+\frac{\pi}{2}$
4	0	0	d_4	$q_4-\frac{\pi}{2}$

TABLE I
Denavit-Hartenberg table for right arm.

There, d_3 equals the length of the arm (from the axis of motor 1 to the axis of motor 4) and d_4 equals the length of the forearm.

B. Dynamics

The elastic joints arm is built from VSA-Cube units (as described in [28]). Here the dynamic of a single unit is modeled by a motor with elastic transmission between the shaft and the link.

We use the simplified model, attributable to [29],

$$\begin{cases} M(q)\ddot{q} + C(q,\dot{q})\dot{q} + g(q) + \tau_m = 0 \\ B\ddot{\theta} + D\dot{\theta} = \tau + \tau_m \\ \tau_m = K(q-\theta) \end{cases} \quad (1)$$

where $M(q)$ is $n \times n$ link inertia matrix, $C(q,\dot{q})$ is a $n \times n$ matrix containing the centripetal and Coriolis terms, $g(q)$ is a $n \times 1$ vector containing the gravity terms, B is a $n \times n$ constant inertia matrix, D is a $n \times n$ matrix modeling viscosity, K is $n \times n$ matrix modeling joint stiffness, q is the $n \times 1$ vector of link joint angles and θ the $n \times 1$ vector of motor shaft angles. In the model K is considered to be linear (which holds true assuming small displacements).

C. The task

The peg-in-hole task consists in inserting a chamfered cylindrical peg in a round hole. The position and orientation of the hole with respect to the peg are uncertain. Since the round peg-in-hole task requires 5DoF to be executed, but each arm only allows for 4DoF manipulation, both arms are used (for a total of 8DoF) to accomplish the task. The peg and hole are fixed to the structure and maintained by the closed hand clamps. The sensory information available in order to resolve the uncertainties and perform the insertion amounts only to the link positions measured by low quality potentiometers: this allows to assess the springs deformation, and consequently the force applied to the end effector, under the assumption that the motor shaft angle is fixed at the commanded position.

III. Problem Solution

The parallel manipulator consisting of the two cooperating arms has been treated as a serial robot as described below.

A search algorithm has been derived in order to resolve uncertainties in the position of the peg and hole and bring the manipulator in a chamfer crossing condition. It is a blind search with the purpose of resolving uncertainties in the hole position along the plane normal to the hole axis. For uncertainties along this axis, a biased approach is used, in that we command a position slightly below the expected chamfer position. The insertion phase is tackled by implementing an induced oscillation motion in order to avoid jamming and accommodating for orientation uncertainties.

A. From parallel to serial manipulation

Joint	a	α	d	θ
1	0	$-\frac{\pi}{2}$	0	q_1
2	0	$\frac{\pi}{2}$	0	$q_2+\frac{\pi}{2}$
3	0	$\frac{\pi}{2}$	$-d_3$	$q_3+\frac{\pi}{2}$
4	0	0	d_4	$q_4-\frac{\pi}{2}$
5	0	$\frac{\pi}{2}$	0	$q_5+\pi$
6	0	$-\frac{\pi}{2}$	0	$q_6-\frac{\pi}{2}$
7	0	$\frac{\pi}{2}$	d_7	$q_7+\frac{\pi}{2}$
8	a_8	0	0	$q_8+\frac{\pi}{2}$

TABLE II
Denavit Hartenberg serial arms.

To invert the kinematics and plan the path of the search and insertion tasks, the parallel manipulation problem has been transformed into an equivalent serial manipulation one by parameterizing the two arms as one serial link, with base reference frame on the right hand and end-effector on the left hand.

In the 8DoF DH table d_3 and a_8 are associated to the right arm, d_4 and d_7 to the left arm.

Expressing the manipulator as a 8DoF serial arm allows to easily derive serial manipulators performance metrics like manipulability ellipsoids. Notice how, for both the search and insertion strategy, 5DoF are required, thus requiring both arms to simultaneously move in a coordinated manner in order to obtain the desired relative position and orientation.

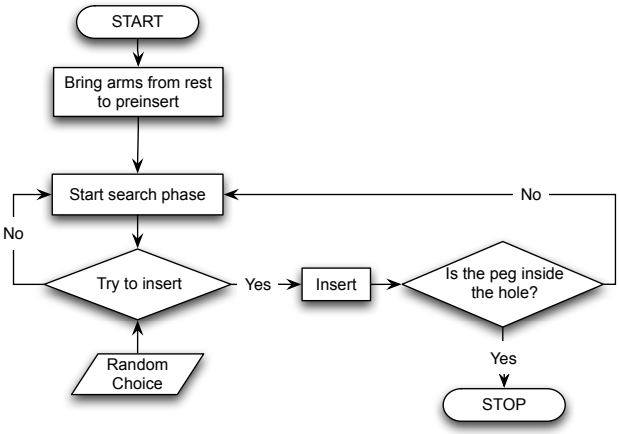

Fig. 4. Search and insert flowchart.

B. Search Algorithm

A search path is pre-calculated using inverse kinematics as defined in the section above.

The search strategy is similar to the technique of the concentric circles from [11]. Two concentric circles of 10mm and 20mm radius are sampled each at 8 equidistant points. The corresponding values for the joint angles are pre-calculated via inverse kinematics and stored in a path file. Inverse kinematics is pre-calculated to avoid computational burden during the task execution. The overall stored path files contains a first part where the arms are brought from a rest position into the pre-insert position (peg tip 10mm above the hole), a search part which contains the 17 points search path (16 circumference points and one point for the circumference center), and a final insertion path consisting of 3 points, with the last one corresponding to the completely inserted peg. All the paths are executed with a constant stiffness preset value, corresponding to the lowest possible stiffness for the VSA-Cube, 3Nm/rad.

Choosing 20mm as the larger radius means we can have a maximum $\sim$30.5mm uncertainty in hole placement, where the uncertainty cap is defined by both the size of the hole crown (having an uncertainty greater than 30.5mm means going out of the crown during the search phase) and the search area (while the center of a 15mm radius peg explores a 20mm radius circle, its center touches at least once the borders of the hole). The search path is executed with a position reference for the peg 10mm inside the hole plane along the insertion axis, so that the peg automatically enters the hole when the two centers happen to be near enough (the required distance is obviously reduced using the chamfered peg) during the search.

Also, the search path is executed by visiting randomly for a certain time all the 8 points in the inner circumference,

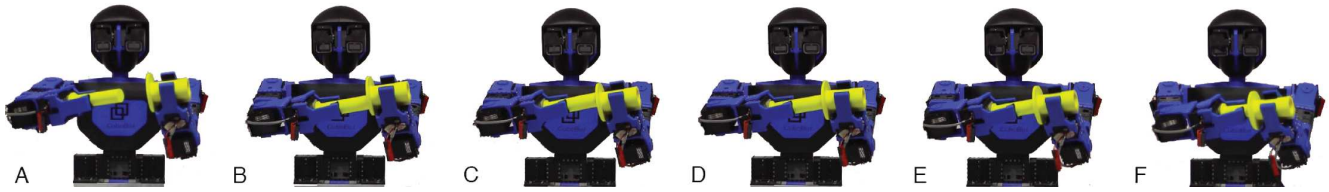

Fig. 3. Search and insertion strategy overview: (A) pre-insert, (B) start search phase, (C) continue searching, (D) trying to insert, (E) vibration and compliance adjust alignment errors, (F) insertion complete

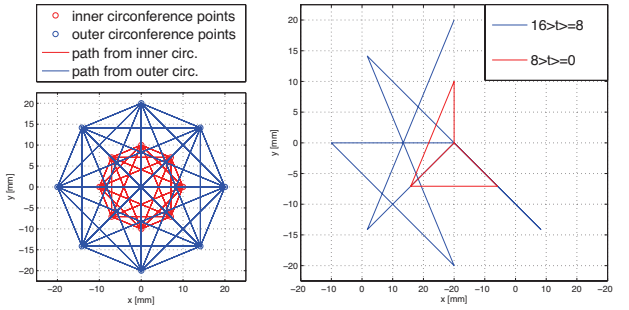

Fig. 5. Complete search path on the left; example of a random walk of random points, from the inner circumference, followed by 8 random point taken from the outer circumference.

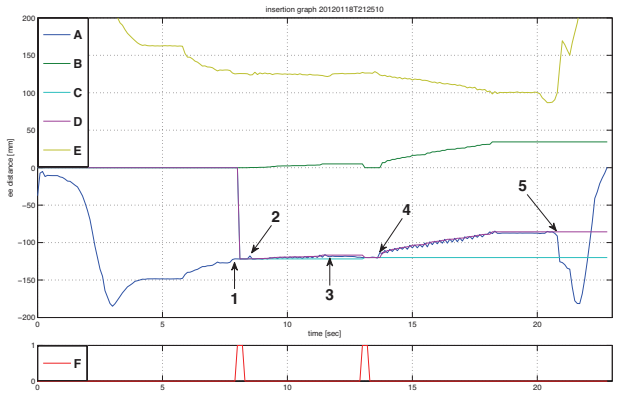

Fig. 6. Insertion check. Legend: A is the z-distance, B is $z_{\text{thrust}} - z_{\text{before}}$, C is z_{before}, D is z_{thrust}, E is the distance between end effectors, F is the logical trigger *insert_start_trigger* which signals the start of the insertion phase. 1 the robot is in the pre-insert position, 2 trying to insert, 3 the insertion phase failed, search is resumed, 4 a new insertion is tried, 5 the insertion has been successfully accomplished, removing peg from hole to return to rest position.

plus the center point, and then switching to the external circumference. Visiting randomly all the circumference points allows for an exploration of the circle area.

During the search phase, the control state machine randomly tries to insert the peg, and checks if it is entering the hole.

C. Insertion

After the search phase the state machine randomly tries to insert the peg another 10mm, while executing an oscillation movement. The thrusts are designed to face three different aspects of the problem:

1) If during the search the peg is partially inside or very near the hole, the insertion and oscillation movement help inserting the peg.
2) It is a way to accommodate for mis-orientations during the insertion phase and resolve jamming conditions.
3) It allows to check if the peg is inside the hole, by analyzing the sensor data against the expected values, obtaining a further proof of a correct peg insertion.

The joint positions measurements are used inside the forward kinematics equation A_s to obtain the Cartesian space coordinates of the hole with respect to the peg.

The insertion check is accomplished by checking that the z-axis coordinate for the hole during the insertion are not greater than the threshold thr_1, and the same coordinate is checked before insertion and during insertion, to see if the difference between the stored z_{before} and the maximum depth reached during thrust z_{thrust} are greater than the threshold thr_2. Both thr_1 and thr_2 are chosen empirically. If t_{check} seconds after the insertion phase the insertion check fails, the search phase is resumed, otherwise the insertion continues for a total of t_{insert} seconds.

The choice of the oscillation movement is very important with respect to the first two aspects, both for correcting orientation errors and to win the insertion frictions. Two approaches were analyzed:

1) oscillations caused by noise applied directly on the joint positions on the axes most relevant to the insertion,
2) oscillations in Cartesian space along the hole x-axis and y-axis, where misalignments are the main cause for the peg to get jammed during insertion.

It must be noted how the insertion path is pre-calculated, which means that the uncertainties regarding the hole position with respect to the peg are not resolved using sensory data, but only taking advantage of joint elasticity. Once the hole is found and the uncertainties relative to its expected position are in this way solved, the insertion tries to proceed as if the hole was in the expected position. It is also worth mentioning that, even though during the insertion phase the stiffness preset have been kept constant to the minimum value possible, the insertion causes a selective stiffness variation along the insertion axis due to the increasing values of $(\theta - q)$ caused by insertion friction.

D. Control

The control used for the task is pure position control. The VSAs are used in their servo mode, where position and stiffness set-points can be imposed. The motor angles are not directly commanded by the central control algorithm.

In this section two regulators are presented which aim to control link positions to a desired constant configuration q_d. For simulation purposes, a simplified model has been used where ODE (the Open Dynamics Engine, see next section for details) is integrated within a Matlab Simulink environment. Joint stiffness is modeled as linear, and input torques for ODE are calculated using the simple equation

$$\tau_m = K(q - \theta) \tag{2}$$

where the θ dynamics is implemented according to the

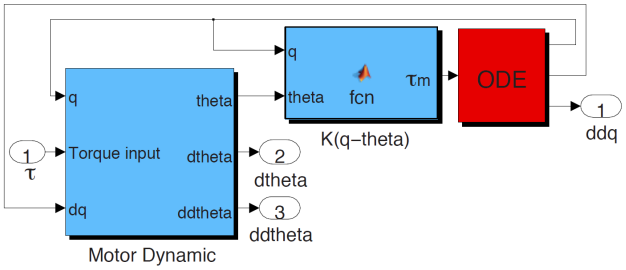

Fig. 7. ODE integration in Simulink.

model (1). This gives us the possibility to apply a torque control with on-line gravity compensation as seen in [30].

$$u = K_p(\theta_d - \theta) - K_d\dot{\theta} + g(q_d) \tag{3}$$

where $K_p \succ 0$ and $K_D \succ 0$ are symmetric, diagonal matrices and

$$\theta_d = q_d + K^{-1}g(q_d) \tag{4}$$

Under the assumption that stiffness matrix K and proportional gain matrix K_p comply with the following condition

$$\lambda_{min}(K) := \lambda_{min}\left(\begin{bmatrix} K & -K \\ -K & K + K_p \end{bmatrix}\right) > \alpha \tag{5}$$

the control law yields global asymptotic stability of the unique closed-loop equilibrium state $(q, \theta, \dot{q}, \dot{\theta}) = (q_d, \theta_d, 0, 0)$. The second control law analyzed is a global PD-type regulator with dynamic gravity cancellation from [31],

$$u = \tau_g + \tau_0 \tag{6}$$

where

$$\tau_g = g(q) + BK^{-1}\ddot{g}(q) \tag{7}$$

$$\tau_0 = K_p(q_d - \theta + K^{-1}g(q)) - K_d(\dot{\theta} - K^{-1}\dot{g}(q)) \tag{8}$$

under minimal sufficient conditions $K_p \succ 0, K \succ 0, K_D \succ 0$ for global asymptotic stability. For this control law knowledge of $\dot{q}$ is necessary. Theoretically the second control scheme allows for better transient response, but its usefulness in the task strategy will be assessed. The VSA-Cubes are stiffness-position servos: the control problem on the real hardware reduces to the computation of θ_d desired motor angles for gravity compensation [32]. The stiffness matrix used for the calculation is considered constant.

IV. Results

Simulations have been conducted using ODE, a quite popular physics engine in the robotics world [33]. Then the task has been executed on the real hardware.

Peter Corke's Robotics Toolbox [34] has been used to pre-calculate the "pre-insert", "search" and "insert" paths using the "ikine" function, which uses a pseudo-inverse Jacobian recursive algorithm; initial position for the ikine algorithm has been provided by manually searching a suitable position considering joint angle limits, arms and body geometry. As hinted above, the Jacobian used for the inverse kinematics calculation is a relative Jacobian.

1) Simulation Environment: An S-Function has been used to simulate the CubeBot with ODE inside Matlab. The motors, elastic transmission and viscosities are simulated in Simulink, together with the motor PD control algorithm with gravity compensation, while the arms, peg and hole physics are completely simulated inside ODE, where the arms are actuated by inputting the total torques exerted by the actuators on the links. While more accurate simulations could be achieved by letting ODE simulate only the collision detections, having a physics environment allows us to validate the control equations against the uncertainties introduced by simulation imperfections. The simulation step time of Simulink and the one used inside of ODE were matched, the ode1 fixed step integration method has been used with an integration time step of .001s.

Parameters for the physic system simulated in ODE match the dynamic model of the system, where the mass of the motors are .26Kg and the viscous friction coefficient on joint axis is 0.55Nms/rad. The dynamic matrices for the system were obtained by using the Robotica package for Mathematica by M. Spong and J. Nethery [35].

2) Experiment: The peg-in-hole task consists of inserting a chamfered 29.5mm diameter cylindrical peg in a 30mm diameter round hole. We assume the height of the peg to be known, measuring 11.5mm. The hole insertion point is slightly above the arm surface, at $\sim$10mm above the motor face normal to the ee z-axis.

Regarding the manipulator, both arm and forearm lengths measure 150mm, each motor size is 55mm. The potentiometers used for measuring link positions have an accuracy of roughly $\pm 5°$.

The right arm carries the peg, with the peg main dimension aligned to right e.-e. x-axis, the hole axis aligned to left e.-e. z-axis. The hole is built with a circular crown of 5mm height and 40mm radius in order to supply a support surface in which the peg can wander in search for the hole. The hole center during grip has a major displacement along the e.-e.

x-axis ($\sim$20mm), while the peg is roughly aligned with the x-axis, with a bigger offsets along the z-axis with respect to the ideal e.-e. position due to the clamps geometry, the peg radius and the non-perfectly rigid grip.

Initial values for the stiffness matrix K were selected according to the data in the VSA-Cube datasheet in [28], selecting the lowest value possible. Some necessary tweaks to the stiffness matrix had to be made due to differences between nominal stiffness and the real one of the actuators. Stiffness values have been corrected with respect to the minimum value by a simple evaluation of the position errors when commanding link angles.

A. Results

Experiments showed that the search strategy is effective, but somehow slow. Since the points on the circumference are visited randomly, without remembering the past followed paths, it can take some time to find the hole when large offsets occur. The attached video reports some experimental trials, one executed in the exact experimental conditions hereby described, the other two in similar but slightly different conditions (details on screen).

The insert strategy proved to be effective. For both noise model, gains for the noise had to be determined: in particular, regarding the induced oscillations, we empirically found the joint axis where the vibrations had the most effect by making the robot execute a motion similar to what a human would have done. Analyzing the variations of the joint axis we determined the gains vector which, in turn, shape the intensity of the oscillations of each joint. The vector of such commanded displacements, which have to be read from shoulder motor to wrist motor, right arm first, are

$$\pm\begin{bmatrix}0 & 1.86 & 0 & 0 & 2.78 & 1.86 & 0.93 & 0\end{bmatrix} \text{ deg}$$

Oscillations during the insertion cause the peg to enter even when the search phase is interrupted and the peg is only near to the hole. Insertion detection required the thresholds thr_1 and thr_2 to be chosen: thr_2 had to be adjusted to the threshold which constitutes an insertion for the biggest peg. Also the times t_{check} and t_{insert} were determined from the worst case scenario, by trying to insert for a longer time before giving up and continuing with the search.

1) Force estimation: Graphics are provided of force estimates during the task. Data from the experiment with minimum stiffness presets and from simulation with stiffness set to 3000Nm/rad are provided. Forces are calculated using the Spong model equations, considering the springs deformation to the effects of external forces on joint torques, and consequently to calculate forces and moments about the end effectors.

$$\tau_{ext} = M(q)\ddot{q} + C(q,\dot{q})\dot{q} + g(q) + K(q-\theta) \qquad (9)$$

For small spring deformations and assuming the motor controls imposes a constant θ, the accuracy of the force estimate is dependent on the accuracy of the model.

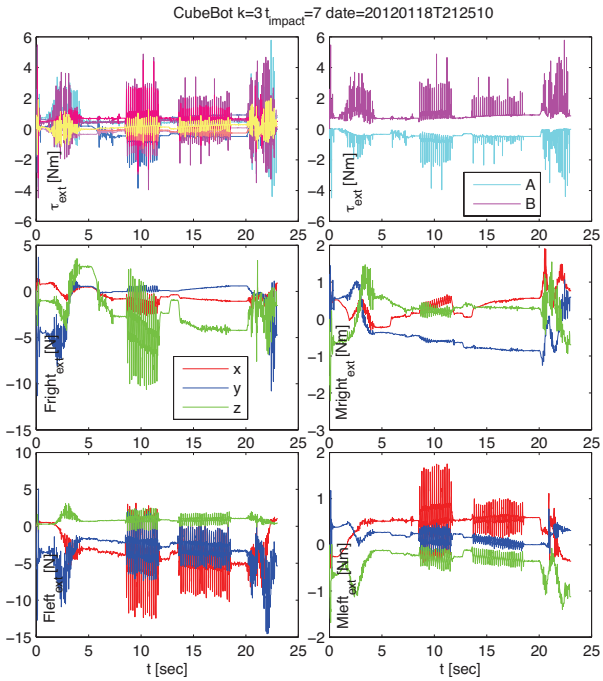

Fig. 8. Forces during the experiment with low stiffness; from t=9 to t=14 the first insertion attempt causes the largest forces; the second insertion is successful, with lower external forces. From left to right, 1) joint torques τ_{ext} , 2) minimum and maximum value for the joint torques with $A = \min(\tau_{\text{ext}})$, $B = \max(\tau_{\text{ext}})$, in the second row 3) forces F_{right} and 4) moments M_{right} along the x, y and z axes and about the e.e. reference base for the right arm, and in the last row the corresponding values 5) F_{left} and 6) M_{left} for the left arm.

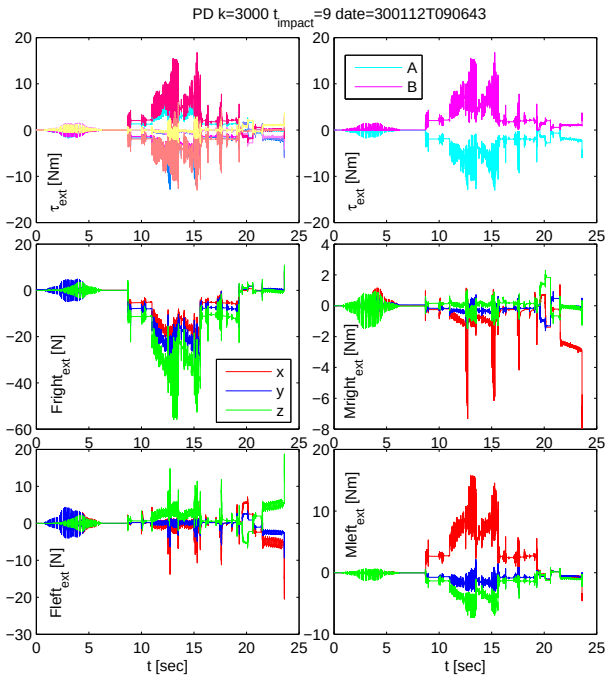

Fig. 9. Forces during the simulation with high stiffness $A = \min(\tau_{\text{ext}})$ $B = \max(\tau_{\text{ext}})$.

V. Conclusions and Future Work

A two arms peg-in-hole task has been demonstrated using a humanoid VSA torso. A simple control algorithm has been chosen, together with a simple search and insertion strategy. Results have been provided both in simulation and real hardware for the insertion strategy performance and contact forces evaluation and are reported also on the attached video.

Acknowledgments

The authors would like to thank Michele Mancini, Fabio Bonomo, Andrea Di Basco and Fabrizio Vivaldi for their valuable aid in the realization of the experimental platform. The research leading to these results has received funding from the European Communitys Seventh Framework Programme (FP7/2007-2013) under grant agreements ICT-287513 “SAPHARI” and FP7 ICT-248587, “THE Hand Embodied”.

References

[1] A. Bicchi, G. Tonietti, and R. Schiavi, “Safe and fast actuators for machines interacting with humans,” in *Proc. First IEEE Technical Exhibition Based Conf. Robotics and Automation TExCRA ’04*, 2004, pp. 17–18.

[2] B.-S. Kim, Y.-L. Kim, and J.-B. Song, “Preliminary experiments on robotic assembly using a hybrid-type variable stiffness actuator,” in *Proc. IEEE/ASME Int Advanced Intelligent Mechatronics (AIM) Conf*, 2011, pp. 1076–1080.

[3] F. Petit and A. Albu-Schaffer, “Cartesian impedance control for a variable stiffness robot arm,” in *Proc. IEEE/RSJ Int Intelligent Robots and Systems (IROS) Conf*, 2011, pp. 4180–4186.

[4] D. Whitney, “Historical perspective and state of the art in robot force control,” in *Proc. IEEE Int. Conf. Robotics and Automation*, vol. 2, 1985, pp. 262–268.

[5] K.-L. Du, B.-B. Zhang, X. Huang, and J. Hu, “Dynamic analysis of assembly process with passive compliance for robot manipulators,” in *Proc. IEEE Int Computational Intelligence in Robotics and Automation Symp*, vol. 3, 2003, pp. 1168–1173.

[6] T. Matsuno, T. Fukuda, and Y. Hasegawa, “Insertion of long peg into tandem shallow hole using search trajectory generation without force feedback,” in *Proc. IEEE Int. Conf. Robotics and Automation ICRA ’04*, vol. 2, 2004, pp. 1123–1128.

[7] M. T. Mason, “Compliance and force control for computer controlled manipulators,” *IEEE*, vol. 11, no. 6, pp. 418–432, 1981.

[8] J. J. Craig and M. H. Raibert, “A systematic method of hybrid position/force control of a manipulator,” in *Proc. IEEE Computer Society’s Third Int. Computer Software and Applications Conf COMPSAC 79*, 1979, pp. 446–451.

[9] N. Hogan, “Impedance control: An approach to manipulation,” in *Proc. American Control Conf*, 1984, pp. 304–313.

[10] H. Asada and Y. Kakumoto, “The dynamic rcc hand for high-speed assembly,” in *Proc. Conf. IEEE Int Robotics and Automation*, 1988, pp. 120–125.

[11] S. R. Chhatpar and M. S. Branicky, “Search strategies for peg-in-hole assemblies with position uncertainty,” in *Proc. IEEE/RSJ Int Intelligent Robots and Systems Conf*, vol. 3, 2001, pp. 1465–1470.

[12] S. kook Yun, “Compliant manipulation for peg-in-hole: Is passive compliance a key to learn contact motion?” in *Proc. IEEE Int. Conf. Robotics and Automation ICRA 2008*, 2008, pp. 1647–1652.

[13] J. F. Broenink and M. L. J. Tiernego, “Peg-in-hole assembly using impedance control with a 6 dof robot,” *Proceedings 8th European Simulation Symposium Simulation in Industry Oct*, pp. 504–508, 1996.

[14] M. Erdmann, “Randomization in robot tasks,” in *Proc. Conf. IEEE Int Robotics and Automation*, 1990, pp. 1744–1749.

[15] M. Okada, S. Ban, and Y. Nakamura, “Skill of compliance with controlled charging/discharging of kinetic energy,” *IEEE Int. Conf. on Robotics and Automation*, pp. 2455–2460, 2002.

[16] B. Vanderborght, B. Verrelst, R. V. Ham, M. V. Damme, D. Lefeber, B. Duran, and P. Beyl, “Exploiting natural dynamics to reduce energy consumption by controlling the compliance of soft actuators,” *Int. Journal of Robotics Research,*, vol. 25, no. 4, pp. 343–358, 2006.

[17] M. Garabini, A. Passaglia, F. Belo, P. Salaris, and A. Bicchi, “Optimality principles in variable stiffness control: The vsa hammer,” in *Proc. IEEE/RSJ Int Intelligent Robots and Systems (IROS) Conf*, 2011, pp. 3770–3775.

[18] M. Garabini, F. A. W. Belo, P. Salaris, A. Passaglia, and A. Bicchi, “Optimality principles in stiffness control: The vsa kick,” in *International Conference of Robotics and Automation - ICRA 2012*, Saint Paul, MN, USA, May 14 - 18 2012, accepted.

[19] S. Haddadin, M. Weis, S. Wolf, and A. Albu-Schäffer, “Optimal control for maximizing link velocity of robotic variable stiffness joints,” in *IFAC World Congress*, 2011.

[20] D. Braun and M. Howard, “Exploiting variable stiffness in explosive movement tasks,” in *roboticsproceedings.org*, 2011.

[21] A. Albu-Schaffer, O. Eiberger, M. Grebenstein, S. Haddadin, C. Ott, T. Wimbock, S. Wolf, and G. Hirzinger, “Soft robotics,” *IEEE Robotics & Automation Magazine*, vol. 15, no. 3, pp. 20–30, Sep. 2008.

[22] M. Mancini, G. Grioli, M. G. Catalano, M. Garabini, F. Bonomo, and A. Bicchi, “Passive impedance control of a qboid multi-dof vsa manipulator,” in *International Conference of Robotics and Automation - ICRA 2012*, Saint Paul, MN, USA, May 14 - 18 2012, accepted.

[23] J. W. Hurst, J. E. Chestnutt, and A. A. Rizzi, “An actuator with physically variable stiffness for highly dynamic legged locomotion,” in *Proc. IEEE Int. Conf. Robotics and Automation ICRA ’04*, vol. 5, 2004, pp. 4662–4667.

[24] B.-S. Kim and J.-B. Song, “Object grasping using a 1 dof variable stiffness gripper actuated by a hybrid variable stiffness actuator,” in *Proc. IEEE Int Robotics and Automation (ICRA) Conf*, 2011, pp. 4620–4625.

[25] ——, “Hybrid dual actuator unit: A design of a variable stiffness actuator based on an adjustable moment arm mechanism,” in *Proc. IEEE Int Robotics and Automation (ICRA) Conf*, 2010, pp. 1655–1660.

[26] Y. Bouffard-Vercelli, P. Dauchez, and X. Delebarre, “Force-controlled assembly with a two-arm robot: How and where to perform it within the workspace,” in *Proc. IEEE/RSJ Int. Conf. Intelligent Robots and Systems ’93 IROS ’93*, vol. 3, 1993, pp. 1977–1984.

[27] J.-D. Choi, S. Kang, M. Kim, C. W. Lee, and J.-B. Song, “Two-arm cooperative assembly using force-guided control with adaptive accommodation,” in *Proc. IEEE/RSJ Int. Conf. Intelligent Robots and Systems IROS ’99*, vol. 2, 1999, pp. 1253–1258.

[28] M. G. Catalano, G. Grioli, M. Garabini, F. Bonomo, M. Mancini, N. Tsagarakis, and A. Bicchi, “Vsa-cubebot: A modular variable stiffness platform for multiple degrees of freedom robots,” in *Proc. IEEE Int Robotics and Automation (ICRA) Conf*, 2011, pp. 5090–5095.

[29] M. Spong, “On the force control problem for flexible joint manipulators,” *Automatic Control, IEEE Transactions on*, vol. 34, no. 1, pp. 107–111, 1989.

[30] S. Nicosia and P. Tomei, “A new approach to control elastic joint robots with application to adaptive control,” in *Proc. 30th IEEE Conf. Decision and Control*, 1991, pp. 343–347.

[31] A. De Luca and F. Flacco, “Dynamic gravity cancellation in robots with flexible transmissions,” in *Proc. 49th IEEE Conf. Decision and Control (CDC)*, 2010, pp. 288–295.

[32] R. Schiavi, G. Grioli, S. Sen, and A. Bicchi, “Vsa-ii: a novel prototype of variable stiffness actuator for safe and performing robots interacting with humans,” in *Proc. IEEE Int. Conf. Robotics and Automation ICRA 2008*, 2008, pp. 2171–2176.

[33] R. Smith, “Ode: Open dynamics engine,” *Online at: http://www. ode. org*, 2003.

[34] P. Corke, “A robotics toolbox for matlab,” *Robotics & Automation Magazine, IEEE*, vol. 3, no. 1, pp. 24–32, 1996.

[35] J. Nethery and M. Spong, “Robotica: a mathematica package for robot analysis,” *Robotics & Automation Magazine, IEEE*, vol. 1, no. 1, pp. 13–20, 1994.